Wide-Band Operation of Microstrip Circulators

Y. S. WU, MEMBER, IEEE, AND FRED J. ROSENBAUM, SENIOR MEMBER, IEEE

Abstract—**Octave bandwidth operation of Y-junction stripline and microstrip circulators is predicted using Bosma's Green's function analysis. The width of the coupling transmission lines is found to be a significant design parameter. Theoretical and experimental results are presented which show that wide lines and a smaller than usual disk radius can be used to obtain wide-band operation. A microstrip circulator is reported which operates from 7–15 GHz.**

Also presented are an analysis of the input impedance and an approximate equivalent circuit for the Y-junction circulator which shows the relationship between Bosma's equivalent circuit and that of Fay and Comstock.

I. INTRODUCTION

THE DESIGN of stripline and microstrip Y-junction circulators is generally based on the works of Bosma [1] and Fay and Comstock [2]. The former uses a Green's function approach to solve the boundary value problem of a ferrite loaded resonator coupled to three transmission lines. The latter gives a phenomenological explanation of circulator operation in terms of the rotation of the magnetic field pattern of the $n = 1$ mode of the resonant junction when it is magnetized in an external field. Experimental measurements [3]–[5] and an assumed equivalent circuit have been used to achieve broad-band operation of circulators by means of impedance matching the junction [6], [7].

Typical designs result in a specification of the center frequency, the geometry, and the ferrite parameters, such that the ratio κ/μ, which describes the anisotropic splitting of the ferrite, is usually small. This leads to narrow band operation of the junction which must then be broad banded using external tuning elements. In this paper octave bandwidth operation of Y-junction circulators is predicated using Bosma's method and demonstrated experimentally. The required junctions are smaller in diameter than usual and the coupling (impedance) transformers are much wider than usual. An explicit equivalent circuit is also developed which shows the equivalence of the results of Bosma and of Fay and Comstock.

Manuscript received January 15, 1974; revised May 8, 1974. This work was supported in part by the Air Force Avionics Laboratory under Contract F33615-72-C-1034, Captain M. Davis, Project Monitor.

Y. S. Wu was with the Department of Electrical Engineering, Washington University, St. Louis, Mo. 63130. He is now with the Central Research Lab., Texas Instruments Incorporated, Dallas, Tex. 75222.

F. J. Rosenbaum is with the Department of Electrical Engineering, Washington University, St. Louis, Mo. 63130.

II. INPUT IMPEDANCE OF Y-JUNCTION CIRCULATOR

Bosma's Green's function approach [1] gives the electric field inside two perfectly conducting parallel disks, completely filled with a ferrite magnetized normal to the disks, that is generated by a unit source $H_\theta = \delta(\theta - \theta')$ located at the edge of the disk. The Green's function for the wave equation satisfied by the electric field is

$$G(r,\theta;R,\theta') = -\frac{jZ_{\text{eff}}J_0(Sr)}{2\pi J_0'(SR)} + \frac{Z_{\text{eff}}}{\pi}\sum_{n=1}^{\infty}\frac{(\kappa/\mu)\,(nJ_n(SR)/(SR))\sin n(\theta-\theta') - jJ_n'(SR)\cos n(\theta-\theta')}{(J_n'(SR))^2 - [(\kappa/\mu)\,(nJ_n(SR)/(SR))]^2}J_n(Sr) \tag{1}$$

where

μ,κ	Polder tensor elements [8] of the ferrite;
$J_n(Sr)$	Bessel function of the first kind with order n;
S	$= (\omega/c)\,(\mu_{\text{eff}}\epsilon_f)^{1/2}$ = radial wave propagation constant;
μ_{eff}	$= (\mu^2 - \kappa^2)/\mu$ = effective permeability of the ferrite;
Z_{eff}	$(\mu_0\mu_{\text{eff}}/\epsilon_0\epsilon_f)^{1/2}$ = intrinsic wave impedance of ferrite;
ϵ_f	relative dielectric constant of ferrite;
$J_n'(Sr)$	derivative of $J_n(Sr)$ with respect to its argument;
r	radial coordinate;
R	disk radius.

The magnetic field is derived from the electric field using Maxwell's equations.

Boundary conditions must now be applied. In general, it is very difficult to effect precise boundary conditions for planar microwave integrated circuits. However, because there are no radial currents at the edge of the conducting disks except at the ports (neglecting fringing), Bosma, Davies and Cohen [9], and others suggest the following boundary condition for the three-port Y-junction circulator shown in Fig. 1:

$$H_\theta = \begin{cases} a, & -\dfrac{\pi}{3} - \psi < \theta < -\dfrac{\pi}{3} + \psi \\ b, & \dfrac{\pi}{3} - \psi < \theta < \dfrac{\pi}{3} + \psi \\ c, & \pi - \psi < \theta < \pi + \psi \\ 0, & \text{elsewhere} \end{cases} \tag{2}$$

where a, b, and c are constants.

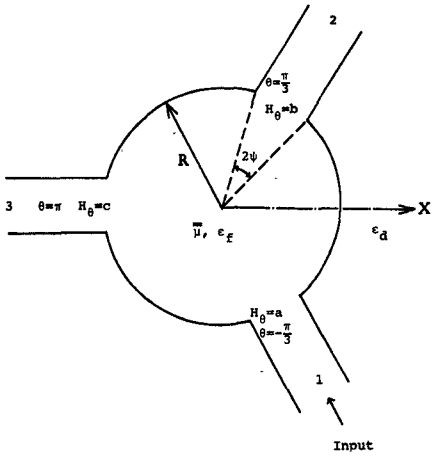

Fig. 1. Junction geometry.

From the above boundary conditions and the Green's function, the total fields can be solved by applying the superposition integral:

$$E_z(r,\theta) = \int_{-\pi}^{\pi} G(r,\theta;R,\theta')H_\theta(\theta')\,d\theta'. \tag{3}$$

Thus from E_z/H_θ, one can derive the input wave impedance Z_{in} and thereby the elements of the scattering matrix for a three-port symmetrical junction:

$$\bar{\bar{S}} = \begin{bmatrix} \alpha & \gamma & \beta \\ \beta & \alpha & \gamma \\ \gamma & \beta & \alpha \end{bmatrix}. \tag{4}$$

The input impedance is

$$Z_{in} = -Z_d - \left(\frac{j2Z_{eff}}{\pi}\right)\left(\frac{C_1^3 + C_2^3 + C_3^3 - 3C_1C_2C_3}{C_1^2 - C_2C_3}\right) \tag{5}$$

where $Z_d = 120\pi/(\epsilon_d)^{1/2}\ \Omega$ and ϵ_d is the relative dielectric constant of medium surrounding the ferrite disk. The scattering matrix elements are

$$\alpha = 1 + \frac{\pi Z_d(C_1^2 - C_2C_3)}{jZ_{eff}(C_1^3 + C_2^3 + C_3^3 - 3C_1C_2C_3)} \tag{6}$$

$$\beta = \frac{\pi Z_d(C_2^2 - C_1C_3)}{jZ_{eff}(C_1^3 + C_2^3 + C_3^3 - 3C_1C_2C_3)} \tag{7}$$

$$\gamma = \frac{\pi Z_d(C_3^2 - C_1C_2)}{jZ_{eff}(C_1^3 + C_2^3 + C_3^3 - 3C_1C_2C_3)} \tag{8}$$

where

$$A_n = J_n'(SR)$$

$$B_n = J_n(SR)$$

$$C_1 = \frac{\psi B_0}{2A_0} + \sum_{n=1}^{\infty}\left(\frac{\sin^2 n\psi}{n^2\psi}\right)\frac{A_nB_n}{A_n^2 - (n\kappa/\mu SR)^2B_n^2} - \frac{\pi Z_d}{j2Z_{eff}} \tag{9a}$$

$$C_2 = \frac{\psi B_0}{2A_0} + \sum_{n=1}^{\infty}\left(\frac{\sin^2 n\psi}{n^2\psi}\right) \cdot \frac{A_nB_n\cos(2n\pi/3) - (jn\kappa/\mu SR)B_n^2\sin(2n\pi/3)}{A_n^2 - (n\kappa/\mu SR)^2B_n^2} \tag{9b}$$

$$C_3 = \frac{\psi B_0}{2A_0} + \sum_{n=1}^{\infty}\left(\frac{\sin^2 n\psi}{n^2\psi}\right) \cdot \frac{A_nB_n\cos(2n\pi/3) + (jn\kappa/\mu SR)B_n^2\sin(2n\pi/3)}{A_n^2 - (n\kappa/\mu SR)^2B_n^2}. \tag{9c}$$

When the circulator is not perfectly matched one can define the return loss, isolation, and insertion loss by

$$\text{return loss} = 20\log_{10}|\alpha| \tag{10a}$$

$$\text{isolation} = 20\log_{10}|\beta| \tag{10b}$$

$$\text{insertion loss} = 20\log_{10}|\gamma|. \tag{10c}$$

The quantity ψ is the half-angle subtended by the coupling transmission lines where they meet the edge of the disk. The resonator is uncoupled when $\psi = 0$. If no impedance transformers are used the circulator is said to be directly coupled, with the input lines having a width $w = 2R\sin\psi$. In this theory ψ is a fundamental design parameter.

Equation (5) contains the variables C_1, C_2, and C_3, which, as indicated in (9), are infinite series. Davies and Cohen [9] consider terms up to $n = 6$ and Whiting [10] even more. In our opinion, since the actual field distribution is smoother than the assumed step function, retaining too many terms does not fit the real situation. On the other hand, retaining only the $n = 1$ mode is also erroneous because the $n = 0$ and $n = 2$ terms play important roles, especially in broad-band circulators [11].

The input wave impedance is calculated from (5), retaining terms up through $n = 3$, and the results shown in Fig. 2. In what follows, the ferrite is just saturated, the applied bias field being approximately $4\pi M_s$, the value of the saturation magnetization. In this case the elements of the Polder tensor are found to be [12], [13]

$$\mu = 1 \tag{11a}$$

$$\kappa = -\frac{\omega_m}{\omega} \tag{11b}$$

$$\omega_m = 2\pi\gamma(4\pi M_s) \tag{11c}$$

where $\gamma = 2.8$ MHz/0e and ω is the microwave radian frequency.

The input wave resistance, normalized to Z_d was calculated for several values of the coupling angle ψ (in radians). As shown in Fig. 2(a), it has two peaks, one at 8.6 GHz and another at 11 GHz for a light coupling angle $\psi = 0.1$. However, when the coupling angle increases

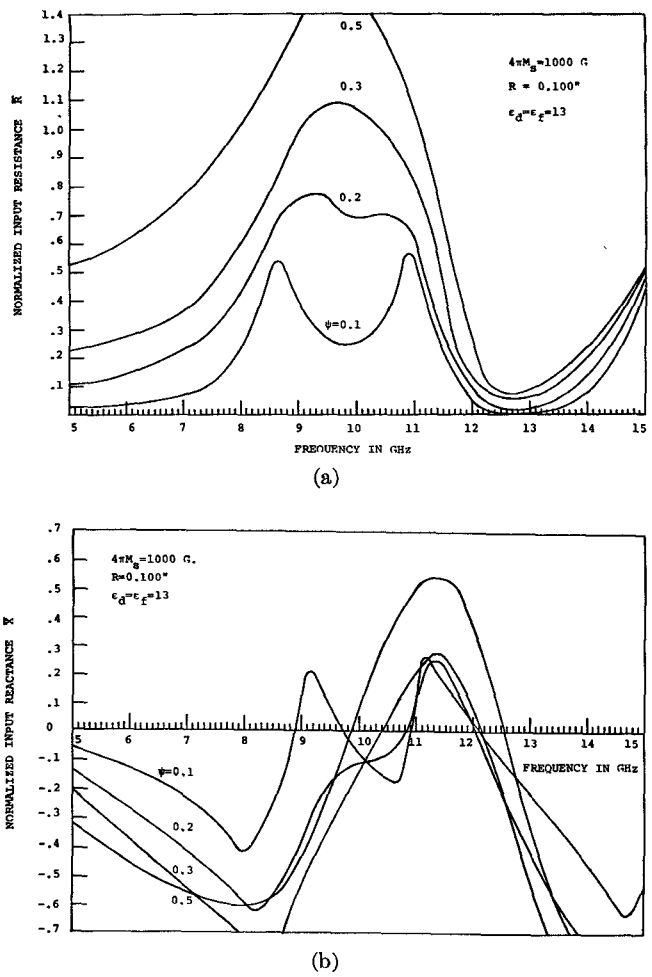

Fig. 2. (a) Normalized input wave resistance of a junction circulator with $4\pi M_s = 1000$ G for various coupling angles. (b) Normalized input wave reactance of a junction circulator with $4\pi M_s = 1000$ G for various coupling angles.

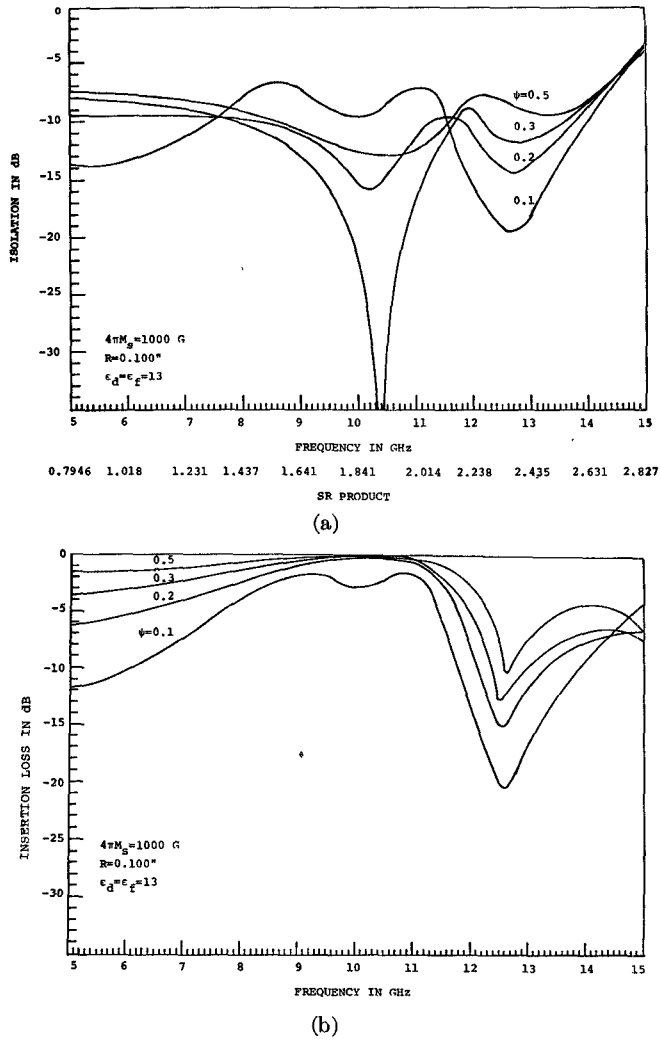

Fig. 3. (a) Calculated isolation for various coupling angles. (b) Calculated insertion loss for various coupling angles.

(tight coupling), the valley between these two peaks becomes flatter and rises. Finally, at $\psi = 0.3$, the two peaks overlap and coalesce to a single peak at $f = 10$ GHz.

Fig. 2(b) shows the corresponding normalized input wave reactances for the above circulators. For a light coupling angle ($\psi = 0.1$), the input reactance is inductive at low frequency ($f < 8.9$ GHz), then capacitive between 8.9 and 9.6 GHz, again inductive for $9.6 < f < 10.9$ GHz, and finally becomes capacitive again at high frequency $f < 10.9$ GHz. These results matched very well with Salay and Peppiatt's [4] and Simon's [3] measurements. The difference in sign of the input reactance of Fig. 2(b) and that of Salay's comes from the negative harmonic $\exp(-j\omega t)$ used here. There are three resonances for $\psi = 0.1$ in Fig. 2(b). The resonances at 8.9 and 11 GHz appear as parallel resonances and the central resonance at 10 GHz is a series resonance. As the coupling angle ψ becomes larger, the two outer resonances move closer to the central resonance. Finally, the reactance becomes that of a parallel R–L–C resonator for tightly coupled circulators.

The input impedance at the band center is of particular importance since this impedance must be matched to the coupling lines if perfect circulation ($\alpha = \beta = 0$, $\gamma = 1$) is required at band center. The center frequency impedance normalized to Z_d can be calculated from (5), retaining the $n = 1$ term only, by noticing that $A_1 = J_1'(x) = 0$ at the band center. It is found to be

$$\bar{Z}_{\text{in}} = \frac{2}{1 + (\psi_c/\psi)^2} \tag{12}$$

where

$$\psi_c = \frac{\pi}{\sqrt{3}(1.84)} \frac{Z_d}{Z_{\text{eff}}} \left| \frac{\kappa}{\mu} \right|$$

is the circulation angle derived by Bosma. Equation (12) shows that the normalized input wave impedance is purely resistive and increases from zero to two when the coupling angle varies from zero to $\psi \gg \psi_c$. When $\psi = \psi_c$, the circulator is matched as predicted by Bosma. When $\psi \neq \psi_c$, the circulator can be matched by applying transformers (6). However, the impedance ratio of the transformer must take (12) into account.

The theoretical performance of the circulator can be calculated from (10). Fig. 3(a) is the calculated isolation

for magnetization $4\pi M_s = 1000$ G, radius $R = 0.100$ in, and dielectric constant $\epsilon_d = \epsilon_f = 13$ for various coupling angles. To get good circulation, the coupling angle should neither be too narrow nor too wide. Here the best result is obtained at $\psi = 0.3$ which is the circulation angle ψ_c. Fig. 3(b) is the insertion loss for various coupling angles. The large insertion loss at low frequencies ($f < 8$ GHz) and high frequencies ($f < 11$ GHz) is due to mismatch (reflection) at the input junction.

III. EQUIVALENT CIRCUIT FOR JUNCTION CIRCULATOR

In order to understand its input impedance and to have an analytical basis for wide-band impedance matching, it is useful to develop an equivalent circuit representation for the junction circulator. For circulators working close to the TM_{110} disk resonance the first order ($n = 1$) term dominates. Thus we may consider this mode alone for the calculation of input impedance as a first order approximation. In (5),

$$C_1 = -2M + jQ \tag{13a}$$

$$C_2 = M + jN \tag{13b}$$

$$C_3 = M - jN \tag{13c}$$

$$M = -\frac{\psi}{2}\frac{A_1B_1}{A_1^2 - (\kappa/\mu SR)^2B_1^2} \tag{13d}$$

$$N = -\frac{\psi}{2}\frac{\sqrt{3}(\kappa/\mu SR)B_1^2}{A_1^2 - (\kappa/\mu SR)^2B_1^2} \tag{13e}$$

$$Q = \frac{\pi Z_d}{2Z_{\text{eff}}}. \tag{13f}$$

Now, consider the input impedance of a series combination of two parallel R–L–C circuits as shown in Fig. 4(a). The input impedance, using $\exp(-j\omega t)$, is [11]

$$Z_{\text{in}} = \frac{1}{(1/R_c) - j(\omega C_+ - 1/\omega L_+)} + \frac{1}{(1/R_c) - j(\omega C_- - 1/\omega L_-)}. \tag{14}$$

Equation (5) is the input impedance of a circulator derived from field theory, while (14) is the impedance of the series combination of two parallel R–L–C circuits. By comparing the results given by the field and circuit approximations, one can derive the following analytic expression for the equivalent circuit elements:

$$R_c = \frac{Z_d}{2}F \tag{15}$$

$$L_\pm = \frac{\psi R\eta}{\pi c}\frac{\mu_{\text{eff}}}{(1 \pm \delta)}F = \frac{L_0}{(1 \pm \delta)}F\ \frac{h}{m} \tag{16}$$

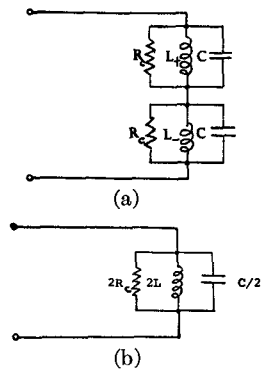

Fig. 4. Equivalent circuit of a junction circulator showing the correspondence between Fay and Comstock's two-resonator model (a) and Bosma's single resonator model (b).

$$C_\pm = \frac{1}{(1.84)^2}\frac{\pi\epsilon_f R}{\psi\eta c}\frac{1}{F} = C_0\frac{1}{F}\ \frac{f}{m} \tag{17}$$

where

η $= 120\pi\ \Omega$ = intrinsic impedance of free space;
R radius of ferrite disk;
c $= 3 \times 10^8$ m/s = speed of light in vacuum;
δ $= \left[\left(\frac{\kappa}{\mu}\right)^2 - \left(\frac{\sqrt{3}\psi SR}{2Q}\right)^2\right]^{1/2}$ = deviation factor; (18)
F geometric factor for the microstrip or stripline characteristic impedance.

Equation (17) shows that the two capacitances are equal and essentially independent of frequency. On the other hand, the two inductances are not the same. For a fixed deviation factor δ, $L_+ < L_0$, and this resonator will have a higher resonance frequency than the L_-C_- one. Both inductances are proportional to the ferrite effective permeability. It is the parallel capacitance which gives bandwidth limitations for broad-band circulators.

For a lightly coupled circulator, ψ approaches zero, so the deviation factor tends to κ/μ, as seen in (18). Referring to Figs. 2(a) and 4(a), the input resistance has two peaks corresponding to the two parallel resonances at $f_\pm = 1/2\pi(L_\pm C_0)^{1/2}$. The higher resonance corresponds to the counterclockwise rotating wave resonance inside the ferrite disk and the lower one corresponds to the clockwise resonance. As the coupling becomes tighter, the deviation factor decreases. Finally, as ψ becomes large enough such that $\kappa/\mu = \sqrt{3}\psi_c SR/2Q$, which is the perfect circulation condition $\psi = \psi_c$, the deviation factor vanishes. In this case, we have $L_+ = L_- = L_0$, and the two resonators are identical. Thus the final equivalent circuit for a circulator at perfect circulation is simply a parallel R–L–C circuit as shown in Fig. 4(b). This is the reason Bosma suggests a single parallel R–L–C resonator for the equivalent circuit of a circulator, while Fay and Comstock suggest Fig. 4(a).

When the coupling angle becomes too large, the deviation factor becomes imaginary. Both the inductances L_+ and L_- are now complex numbers and the equivalent circuit loses its physical meaning.

IV. DESIGN OF A WIDE-BAND CIRCULATOR

To get perfect circulation, one of the three ports must be completely isolated. Mathematically, this can be achieved by setting β in the scattering matrix equal to zero. From (7) we can write

$$C_2^2 = C_1 C_3. \tag{19}$$

Since C_1, C_2, C_3 are complex numbers, (19) can be decomposed into the following two conditional equations:

$$\text{(A)} \quad P = \frac{M(M^2 - 3N^2)}{(M^2 + N^2)} \tag{20}$$

$$\text{(B)} \quad Q = \frac{N(3M^2 - N^2)}{(M^2 + N^2)} \tag{21}$$

where

$$P = \text{Re}\,(C_1) = \frac{\psi B_0}{2A_0} + \sum_{n=1}^{\infty} \frac{\sin^2 n\psi}{n^2\psi} \frac{A_n B_n}{A_n^2 - (n\kappa/\mu SR)^2 B_n^2}$$

$$Q = \text{Im}\,(C_1) = \frac{\pi Z_d}{2Z_{eff}}$$

$$M = \text{Re}\,(C_2) = \frac{\psi B_0}{2A_0} + \sum_{n=1}^{\infty} \left(\frac{\sin^2 \psi}{n^2\psi}\right) \frac{A_n B_n \cos(2n\pi/3)}{A_n^2 - (n\kappa/\mu SR)^2 B_n^2}$$

$$N = \text{Im}\,(C_2) = \sum_{n=1}^{\infty} \left(\frac{\sin^2 n\psi}{n^2\psi}\right) \frac{(n\kappa/\mu SR) B_n^2 \sin(2n\pi/3)}{A_n^2 - (n\kappa/\mu SR)^2 B_n^2}.$$

Equations (20) and (21) are the two conditions required for perfect circulation. They are essentially the same conditions as derived by Davies and Cohen [9]. As shown earlier, the quantities P, M, and N are infinite series with each term corresponding to a particular resonator mode. These infinite terms are necessary for the circulator to satisfy the particular boundary conditions. However, not all terms are important in practical application. Since most circulators operate close to the $n = 1$ resonance, many people consider only the $n = 1$ term and the above two conditions reduce to

$$SR = 1.84 \tag{22a}$$

$$\psi = \frac{\pi}{\sqrt{3}(1.84)} \frac{Z_d}{Z_{\text{eff}}} \left|\frac{\kappa}{\mu}\right|. \tag{22b}$$

Fig. 5 shows the computed perfect circulation roots from (20), retaining terms up to the third order. The roots were sought from $SR = 0$ through $SR = 3.0$. There are two sets of results. One, specified by mode 1+, is the mode 1A mentioned by Davies and Cohen. The other set is the usual circulation root which is concentrated at $SR = 1.84$ for small values of $|\kappa/\mu|$. Since the mode 1+ solutions require a larger disk and also need a large impedance ratio between the substrate and the disk [9], this mode is not practically suitable. As shown by Davies and Cohen there is a further set of roots between the 1+ and 1− modes, corresponding to the middle zero of the $\psi = 0.1$ curve in Fig. 2(b), at 9.6 GHz.

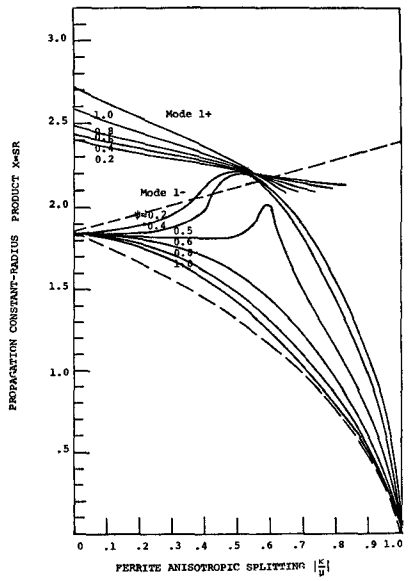

Fig. 5. Perfect circulation roots of the first circulation condition for various coupling angles (third order).

Therefore, we will pay special attention to the lower solution. The dashed curves are the roots of the uncoupled resonator. For lightly coupled circulators ($\psi < 0.4$), the roots first increase with increasing $|\kappa/\mu|$ and then decrease. On the other hand, for tightly coupled ($\psi > 0.5$) circulators, the roots start going down even for small $|\kappa/\mu|$. This phenomena is noticed by circulator designers [13], [14], but is not predicted by Davies and Cohen and Whiting. Massé [14] noticed that his broad-band circulator requires a radius about 7.5 percent less than the predicted design. He suggests that this is caused by fringing fields. In addition to this, the calculations here show that higher order modes (especially $n = 2$) have a significant effect in shrinking the required circulator radius.

Fig. 6 is the second circulation condition which is found

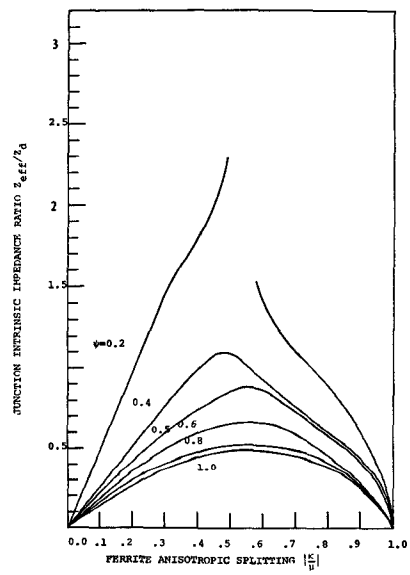

Fig. 6. Normalized junction impedance ratio as a function of anisotropic splitting factor calculated from the second circulation condition for various coupling angles.

by substituting the roots obtained from (20) into (21). The second condition gives the dielectric and disk wave impedance ratio at the junction. Both circulation conditions must be satisfied to get perfect circulation.

Since the two conditions for circulation are known, the design of a direct coupled circulator becomes a simple task. The first step is to choose the ferrite material and the dielectric medium. This is easily achieved in stripline. By using arc plasma spray (APS) [15] methods, or by inserting a ferrite puck into a hole in the substrate these choices can be made independently in microstrip. The second step is to plot the impedance ratio curve as a function of $|\kappa/\mu|$. The third step is to choose the coupling angle and get the intersection point of the impedance ratio curve and the corresponding curves in Fig. 6. Then the operating point $|\kappa/\mu|$ is specified (condition 2) from the abscissa of the intersection point. The final step is to determine the circulator radius from the corresponding point found in Fig. 5 (condition 1).

In the design of a circulator, one tries to find the intersection of the following two curves.

a) The impedance ratio Z_{eff}/Z_d of the chosen puck and dielectric material.

b) The calculated impedance ratio of the second circulation condition given in Fig. 6.

However, the condition 2 curves shown in Fig. 6 have a general property; all curves have positive slope with increasing $|\kappa/\mu|$ when $|\kappa/\mu| < 0.5$ and negative slope when $|\kappa/\mu| > 0.5$. For a weakly magnetized ferrite, operated below resonance, the impedance ratio is approximately given by

$$\frac{Z_{\text{eff}}}{Z_d} = \left(\frac{\epsilon_d}{\epsilon_f}\right)^{1/2}\left(1 - \left(\frac{\kappa}{\mu}\right)^2\right)^{1/2}. \tag{23}$$

This impedance ratio is shown for $\epsilon_d/\epsilon_f = 1$ in Fig. 7. As indicated, this curve always has a negative slope. Thus when $|\kappa/\mu|$ at the center frequency is less than 0.5, there is only one intersection near $|\kappa/\mu| \approx 0.2$ for $\psi = 0.2$. In this case a circulator with fixed radius works only in a limited frequency range. Even with quarter-wave transformers the bandwidth is still limited to about 25 percent [2], [6]. However, when $|\kappa/\mu|$ is greater than 0.5, both the impedance ratio curves and condition 2 curves have the same negative slope. Thus there can be a continuous solution if appropriate coupling angle and materials are selected.

For example, a special case is also shown in Fig. 7. The impedance ratio curve for $\epsilon_d/\epsilon_f = 1$ is plotted as a function of $|\kappa/\mu|$, along with the condition 2 curve for $\psi = 0.51$. As shown in the figure, there is no intersection for $|\kappa/\mu| < 0.5$. However, these two curves nearly overlap for $0.5 < |\kappa/\mu| < 1.0$. This means that for this particular design, the circulator not only works at $|\kappa/\mu| = 0.5$, but all the way from $|\kappa/\mu| = 0.5$ to $|\kappa/\mu| = 1.0$. Thus, as seen from Fig. 8, it can be used, in principle, from $SR = 0$ up to $SR \approx 1.84$. The importance of this phenomena is that the regular single intersection circulator can be replaced

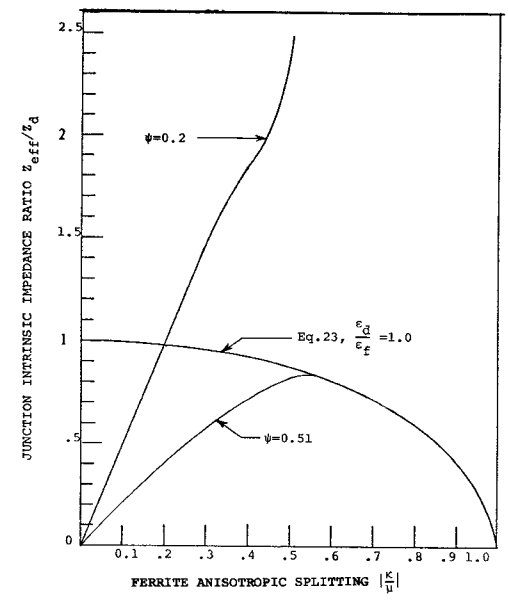

Fig. 7. Comparison of junction wave impedance ratio from the second circulation condition and from (23), as a function of $|\kappa/\mu|$.

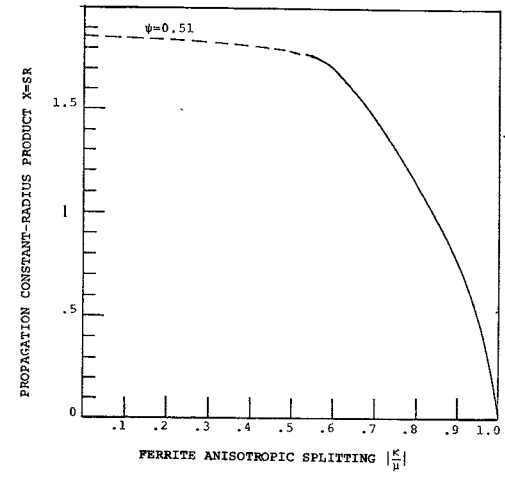

Fig. 8. Operating range of a continuous tracking circulator.

by an inherently broad-band circulator whose operating range is from $|\kappa/\mu| = |\omega_m/\omega| = 1$ or $\omega_L = \omega_m$ to $|\kappa/\mu| = |\omega_m/\omega| = 0.5$ or $\omega_H = 2\omega_m$. The bandwidth $(\omega_H - \omega_L)$ is approximately $\omega_m/2\pi = f_m = \gamma(4\pi M_s)$. An octave bandwidth circulator can be easily achieved according to this theory.

Notice that $SR = 0$ does not mean zero frequency. Since the radial wave propagation constant S is given by $S = (\omega/c)(\mu_{\text{eff}}\epsilon_f)^{1/2}$, the lower frequency which corresponds to $SR = 0$ is the one which yields $\mu_{\text{eff}} = 0$. For a ferrite just saturated, this frequency is given by $f = \gamma(4\pi M_s)$. However, because of low field losses, the actual operation band cannot reach $\mu_{\text{eff}} = 0$ or $|\kappa/\mu| = 1$.

To prove the existence of such a broad-band circulator, a microstrip device was fabricated using the structure shown in Fig. 9. The circulator radius is 0.100 in and the junction coupling angle is $\psi \simeq 0.525$ rad. The ferrite

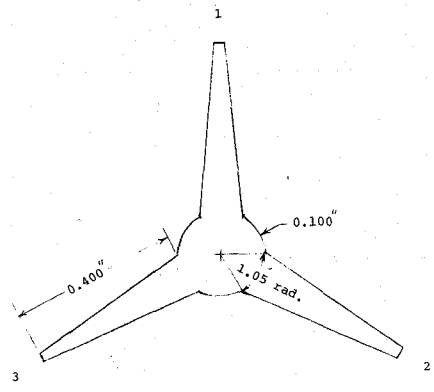

Fig. 9. Sample conductor pattern for a continuous tracking circulator.

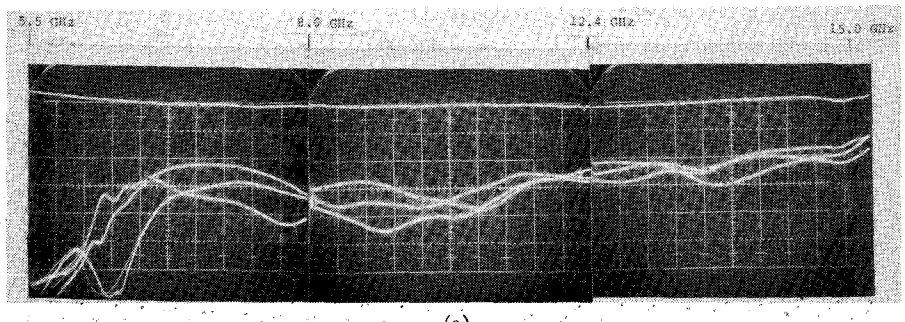

(a)

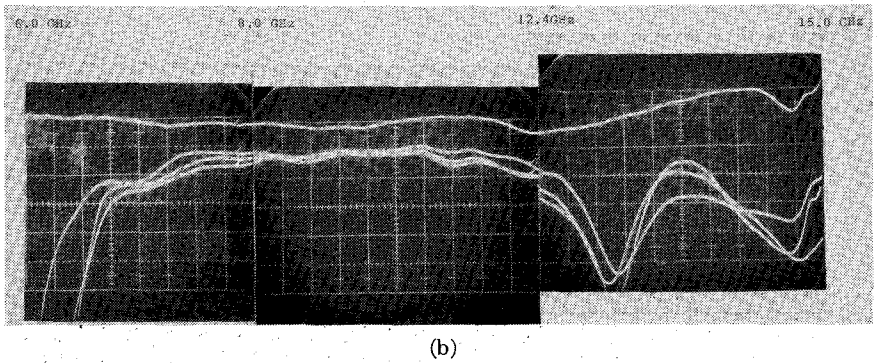

(b)

Fig. 10. Performance of an experimental continuous tracking circulator. (a) Isolation scale: 5 dB/div. (b) Insertion loss: scale: 1 dB/div.

material was TT1-390 which has a saturation magnetization of 2150 G (f_m = 6.02 GHz). The circulator is matched by a linear transformer to each of three 50-Ω microstrip lines on the same ferrite substrate. This linear transformer should be at least one wavelength long to get a good match.

Fig. 10(a) shows the experimental isolation for each of the three input ports, measured sequentially. The frequency range covered is from 5.5 to 15.0 GHz. The scale is 5 dB/div with the top line as the reference. It is seen that an average isolation of about 15 dB is obtained over the range 7–12.4 GHz. The resonance loss and cutoff region is obvious in the photograph below 6 GHz. The operating Bessel function argument SR runs from 0 up to 1.84. This follows, approximately, our prediction from Fig. 8. The center frequency is located at 9 GHz (SR = 1.2).

Although the device operates with large $|\kappa/\mu|$, the insertion loss shown in Fig. 10(b) is less than 1.0 dB over the range. The device was biased top and bottom with 0.2-in-diameter magnets, about 3/8 in tall. The large absorption shown near 13.2 GHz is caused by radiation from the top magnet.

V. CONCLUSION

These experimental results suggest that microstrip Y-junction circulators with bandwidth of the order of (2.8 MHz/Oe) × ($4\pi M_s$) can be readily fabricated simply by choosing the appropriate (wide) coupling angle and disk radius ($SR \approx 1.2$) and then suitably connecting to the 50-Ω input lines. Improved performance should be obtained through the use of a thick substrate such that the direct coupled 50-Ω lines are already as wide as the

required coupling junction width. When using thin substrates, the isolation obtainable over the band will depend on the impedance characteristics of the transformers chosen. The quality of the terminations, connectors, and homogeneity of the biasing magnets are also very important as in any circulator design. This experiment gives good evidence of the existence of such a broad-band circulator.

The model presented here gives an improved understanding of the design and operation of circulators in the following ways. The input impedance of a circulator is analyzed rigorously using a Green's function approach. The equivalent circuit of the junction circulator is found to be a series combination of two parallel *RLC* circuits which reduce to a single resonator when the conditions for perfect circulation are achieved. Thus the equivalence between Bosma's model and that of Fay and Comstock is shown.

A continuous tracking technique is discovered which makes the fabrication of octave bandwidth circulators straightforward. This circulator is recognized [16] by: a) wide coupling angle $\psi \simeq 0.5$, and b) smaller than usual circulator radius; center frequency of operating band is found from $SR \approx 1.2$.

ACKNOWLEDGMENT

The authors wish to thank Dr. M. Davis, now of General Electric Company, and D. H. Harris of the Monsanto Research Corporation, Dayton, Ohio, for their interest, support, and encouragement; R. West of Trans-Tech for the substrates; and Dr. R. H. Knerr of the Bell Laboratories for metallizing and etching the substrates.

REFERENCES

[1] H. Bosma, "On stripline *Y*-circulation at UHF," *IEEE Trans. Microwave Theory Tech.* (*1963 Symposium Issue*), vol. MTT-12, pp. 61–72, Jan. 1964.
[2] C. E. Fay and R. L. Comstock, "Operation of the ferrite junction circulator," *IEEE Trans. Microwave Theory Tech.* (*1964 Symposium Issue*), vol. MTT-13, pp. 15–27, Jan. 1965.
[3] J. W. Simon, "Broadband strip-transmission line *Y*-junction circulators," *IEEE Trans. Microwave Theory Tech.*, vol. MTT-13, pp. 335–345, May 1965.
[4] S. J. Salay and H. J. Peppiatt, "Input impedance behavior of stripline circulator," *IEEE Trans. Microwave Theory Tech.* (Corresp.), vol. MTT-19, pp. 109–110, Jan. 1971.
[5] ——, "An accurate junction circulator design procedure," *IEEE Trans. Microwave Theory Tech.* (Corresp.), vol. MTT-20, pp. 192–193, Feb. 1972.
[6] L. K. Anderson, "An analysis of broadband circulators with external tuning elements," *IEEE Trans. Microwave Theory Tech.*, vol. MTT-15, pp. 42–47, Jan. 1967.
[7] E. Schwartz, "Broadband matching of resonant circuits and circulators," *IEEE Trans. Microwave Theory Tech.*, vol. MTT-16, pp. 158–165, Mar. 1968.
[8] D. Polder, "On the theory of ferromagnetic resonance," *Phil. Mag.*, vol. 40, pp. 99–115, Jan. 1949.
[9] J. B. Davies and P. Cohen, "Theoretical design of symmetrical junction stripline circulator," *IEEE Trans. Microwave Theory Tech.*, vol. MTT-11, pp. 506–512, Nov. 1963.
[10] K. Whiting, "Design data for UHF circulators," *IEEE Trans. Microwave Theory Tech.* (Corresp.), vol. MTT-15, pp. 195–198, Mar. 1967.
[11] H. Bosma, "Junction circulators," in *Advances in Microwaves*, vol. 6, L. Young, Ed. New York: Academic, 1971.
[12] E. Schlömann, "Microwave behavior of partially magnetized ferrites," *J. Appl. Phys.*, vol. 41, pp. 204–214, Jan. 1970.
[13] D. J. Massé and R. A. Pucel, "Microstrip propagation on magnetic substrates—Part II: Experiment," *IEEE Trans. Microwave Theory Tech.*, vol. MTT-20, pp. 309–313, May 1972.
[14] D. J. Massé, "Broadband microstrip junction circulators," *Proc. IEEE* (Lett.), vol. 56, pp. 352–353, Mar. 1968.
[15] D. H. Harris *et al.*, "Polycrystalline ferrite films for microwave applications deposited by arc-plasma," *J. Appl. Phys.*, vol. 41, pp. 1348–1349, Mar. 1970.
[16] Y. S. Wu and F. J. Rosenbaum, "Ferrite/dielectric high power phase shifter development—Part II on broadband *Y*-junction circulators," Air Force Avionics Lab., Air Force Systems Command, Wright-Patterson Air Force Base, Ohio, Tech. Rep. AFAL-TR-73-250, pt II.